Available online at www.sciencedirect.com
ScienceDirect
Polymer 48 (2007) 1695–1710
polymer
www.elsevier.com/locate/polymer

Cure kinetics, morphology and miscibility of modified DGEBA-based epoxy resin – Effects of a liquid rubber inclusion

Raju Thomas [a], Sebastien Durix [b], Christophe Sinturel [b], Tolib Omonov [c], Sara Goossens [d], Gabriel Groeninckx [d], Paula Moldenaers [c], Sabu Thomas [e,*]

[a] *Department of Chemistry, Mar Thoma College, Tiruvalla 689103, Kerala, India*
[b] *Centre de Recherche Sur la Matiere Divisee, Universite d'Orleans, France*
[c] *Department of Chemical Engineering, Catholic University of Leuven, de Croylaan 46, B-3001 Leuven, Belgium*
[d] *Laboratory of Macromolecular Structural Chemistry, Catholic University of Leuven, Celestijnenlaan 200F, 3001 Haverlee, Belgium*
[e] *School of Chemical Sciences, Mahatma Gandhi University, Priyadarshini Hills P.O., Kottayam 686560, Kerala, India*

Received 5 August 2006; received in revised form 4 January 2007; accepted 12 January 2007
Available online 17 January 2007

Abstract

Kinetics of the curic reaction and morphology of a diglycidyl ether of bisphenol-A based epoxy resin (DGEBA), using an anhydride hardener (nadic methyl anhydride) at different weight contents of carboxyl-terminated copolymer of butadiene and acrylonitrile liquid rubber (CTBN) was investigated using a differential scanning calorimetry (DSC), dynamic mechanical thermal analysis (DMTA), and scanning electron microscopy (SEM). The aim of the work is to understand the effects of inclusion of the liquid rubber phase in the transition phenomena that occur during the curing reaction. The curic reaction at three different curic temperatures and at varying rubber contents in the range of 5–20 wt% has been studied. The reaction rate and conversions that occurred at the curic temperatures were analyzed. The increase in the rate with the curic temperature showed this as a thermally catalyzed reaction. The rate of the reaction was found to decrease in liquid rubber-modified epoxies due to the effect of dilution and viscosity increase as obtained from the gelation times. The experimental data showed an autocatalytic behavior of the reaction, which is explained by the model predicted by Kamal. This model includes two reaction constants k_1 and k_2 and two reaction orders m and n. The order of the overall reaction was found to be approximately 2. The activation energies Ea_1 and Ea_2 were estimated at all curic temperatures for neat and all modified epoxies. The results obtained from the DSC data were also applied to diffusion controlled kinetic models. A schematic model to represent the curic reaction and phase separation was introduced and the molecular mechanism of this curing reaction was discussed. During the curic reaction, phase separation of the liquid rubber from the epoxy matrix took place and the modified epoxies showed phase separated morphology. The dispersed phase showed a homogenous particle size distribution. The size of the phase separated domains increased with increasing concentration of the CTBN and decreased with rise in curing temperature. The glass transition temperature (T_g) of the modified epoxies decreased with increase in curic temperature as studied from dynamic mechanical thermal analysis. Addition of the liquid rubber lowered the T_g of the network. This became prominent in the modification of the matrix with 15 and 20 wt% of the elastomer. This is attributed to flexibilization of the matrix. The dissolved rubber plasticizes the epoxy network. The T_g of the neat rubber in the low-temperature region was shifted to higher temperature upon addition of the elastomer. A higher shift was noted for 15 and 20 phr inclusion. This was due to dissolved epoxy in the rubber-rich phase that increased the modulus of the rubbery phase. The inclusion of a large wt% of carboxyl-terminated butadiene-*co*-acrylonitrile (CTBN) decreased the cross-linking density of the thermoset matrix.

Keywords: Epoxy resin/liquid rubber; DSC; Cure kinetics

* Corresponding author. Tel.: +91 481 2730003; fax: +91 481 2561190.
E-mail addresses: sabut@sancharnet.in, sabut552001@yahoo.com (S. Thomas).

0032-3861/$ - see front matter © 2007 Elsevier Ltd. All rights reserved.
doi:10.1016/j.polymer.2007.01.018

1. Introduction

Epoxy resins are widely used as high-performance protective coatings, structural adhesives, low-stress IC encapsulants, and matrix resins for composites. When cured these resins are highly cross-linked and become amorphous thermosets. They are brittle and have poor resistance to crack growth. They are highly employed in ''joining and fastening technology'' in many industries. The epoxy resin network is formed during the cross-linking reaction using a wide variety of cross-linking agents or hardeners such as acids [1], anhydrides [2], and amines [3]. The reaction leads to the formation of a three-dimensional system which is found to be insoluble in usual solvents.

Toughening of epoxy resins with low-molecular weight liquid rubbers has been studied [4–8]. Many authors [9–11] have also made comments on the increasingly wide use of rubber-modified epoxy resins as structural adhesives and as the matrix for fiber composites. Because of their properties, epoxy resins have many commercial applications. For this reason, it was deemed interesting to modify them with rubber particles. Rubber was added to the uncured epoxy resins and after the cross-linking reactions the rubber-modified epoxy resins exhibited a two-phase microstructure consisting of relatively small rubber particles dispersed in a matrix of epoxy. This microstructure resulted in the material possessing a higher toughness than the unmodified one with only a minimal reduction in other important properties, such as modulus. Toughening of epoxy resin is extremely useful because application of this polymeric material imparts resistance against mechanical deformation at different loading rates. The brittle nature of the epoxy is the result of catastrophic strain localization in the form of crazes, which may cause premature fracture at a relatively small macroscopic deformation. Microstructural adjustments in the system resulted in the introduction of heterogeneity in polymer systems [12]. Rubber toughening [13] or cross-linking [14] of epoxy system results in the increase in hardening modulus.

The properties of the epoxy resin depend on the extent of reaction. The knowledge of the mechanism and cure kinetics is necessary for assigning structure–property relationships and for the usage of the materials as structural adhesives and as matrices in fiber-reinforced composite. Generally the curing of the epoxy resin is studied by DSC [15–18]. This calorimetric technique gives a quantitative measurement on the amount of reaction and permits to determine the T_g of the material. Cure kinetics of the epoxy–anhydride system has been studied using various non-isothermal DSC scans, and hence the calculation of activation energy has been done by many authors [19,20]. Certain studies deal with cure kinetics of a DGEBA epoxy resin in the presence of sulfanilamide (SAA) at different heating rates by non-isothermal DSC [21]. Francis et al. have studied the cure kinetics of DGEBA-based epoxy resin modified with an engineering thermoplastic, i.e. poly(ether ether ketone) with diaminodiphenyl sulfone (DDS) curing agent using isothermal DSC, SEM, and DMTA [22]. Non-isothermal DSC technique was employed by Rosu et al. in a cure kinetic study of DGEBA and diglycidyl ether of hydroquinone (DGEHQ) epoxy resin using triethylenetetramine (TETA) as the curing agent [23]. Near-infrared (NIR) spectroscopy was also employed to analyze the cure kinetics of tetraglycidyl-4,4′-diaminodiphenyl methane with DDS as a curative [24]. Cure kinetics, using isothermal mode of DSC was employed to study a system composed of *o*-cresol formaldehyde epoxy resin (*o*-CFER) using succinic anhydride (SA) as the curative and a tertiary amine as a catalyst [25]. In a certain study by Raman and Palmese, Fourier transform infrared (FTIR) spectroscopy in the NIR region was used to monitor the cure kinetics of DGEBA epoxy resin and 4,4′-methylenebiscyclohexanamine in the presence of THF as a solvent [26]. DGEBA and aniline modified with a low-T_g poly(ethylene glycol) (PEG) were used as a model system to study the importance of complex formation on the cure kinetics of multicomponent epoxy-amines [27]. In another study, wide-angle X-ray analysis (XRD) was carried out at different stages of cure to monitor the kinetics of di-, tri-, and tetra-functional high-performance, epoxy-layered silicate nanocomposites [28]. Different techniques including DSC, FTIR, and transmission electron microscopy (TEM) have been used to demonstrate the curic reaction of epoxy thermoset and a block copolymer modifier synthesized from polystyrene, polybutadiene, and poly(methyl methacrylate) incorporated by an acid-reactive functionality [29].

The inclusion of elastomers on epoxy resin results in a phase separated network on curing. However, there are several reports on DGEBA-based epoxy resin and elastomeric modified blends on immiscibility or miscibility depending on the structure of the curing agent. In a very recent interesting investigation by Kalogeras et al. [30], aromatic amine-cured DGEBA epoxy resin and poly(ethylene oxide) (PEO) blends were analyzed by DSC and dielectric techniques to study the parameters controlling miscibility. In another recent work [31], miscibility parameters were analyzed by DSC for ternary thermosetting blends composed of epoxy resin, PEO, and poly(ε-caprolactone) (PCL).

The epoxy curing generally shows a complex kinetics. Autocatalysis is the reason for initial acceleration. But due to the onset of gelation, the reaction retards in the next stage. The cross-linking leads to an increase in the T_g of the curing matrix. If the curic temperature (T_{cure}) is well above T_g, the kinetics of the reaction between epoxy and hardener is chemically controlled. The resin passes from a flexible rubbery state to a rigid glassy one, when T_g approaches T_{cure}. The reaction, at this stage, becomes very slow, only diffusion controlled, and finally attains vitrification stage and stops.

Many studies have been published on the cure kinetics of DGEBA-based epoxy resin with carboxyl-terminated liquid rubber. Also, calorimetric method by DSC was employed in most of the works. The curic reaction takes place between the epoxy and the curative and hence the kinetics depends on the nature of the hardener employed. Thus, each system can be considered as a separate entity depending on the type of curative used. The significance of the present study lies in the investigation of cure kinetics of the DGEBA-based epoxy

resin with carboxyl-terminated liquid rubber using an anhydride as the curative. This keeps the system odd from others and a new one to report cure kinetics to the best of our knowledge. In the present case, a cyclic anhydride, nadic methyl anhydride, was used as the hardener. DSC in isothermal mode was employed for the calorimetric analysis. The kinetics of the first stage of the reaction as well as the later stages where the vitrification effect is dominant and controlled by diffusion instead of chemical kinetics has been explained. The effect of the reactive liquid rubber, carboxyl-terminated butadiene-*co*-acrylonitrile (CTBN), inclusion of varying weight content on the epoxy system has also been checked. The morphological development during the cure processes was also analyzed. The viscoelastic behavior of the modified epoxies was analyzed using DMTA.

2. Experimental

2.1. Materials

The epoxy resin used was a diglycidyl ether of bisphenol-A (DGEBA, Gy-250). The curing agent was an anhydride, nadic methyl anhydride, under the trade name Hy-906. A tertiary amine, *N*,*N*-dimethyl benzylamine (Dy-062), was used as an accelerator. The liquid rubber used was the carboxyl-terminated butadiene-*co*-acrylonitrile (CTBN), Hycar 1300*8. All the chemicals were kindly supplied by Huntsmann Co. and were used as received without purification. Fig. 1 shows the structures of the materials used in the study. The characteristics of CTBN rubber are summarized in Table 1. The stoichiometry of epoxy and anhydride is 5:4. The mixture was stirred at room temperature and samples of about 15–20 mg weights were analyzed.

2.2. Blend preparation

Solutions of varying CTBN concentrations in the epoxy resin were prepared by agitating the mixture using a mechanical stirrer at room temperature. Stoichiometric amount of anhydride was added followed by the tertiary amine accelerator. Small amounts of samples taken from freshly prepared blends were used for DSC analysis. For SEM analysis blended samples were prepared by pouring the mixture into a preheated silicone mould. It was then precured under ambient conditions for 30 min at 120 °C and then postcured for 2 h at 140 and 150 °C.

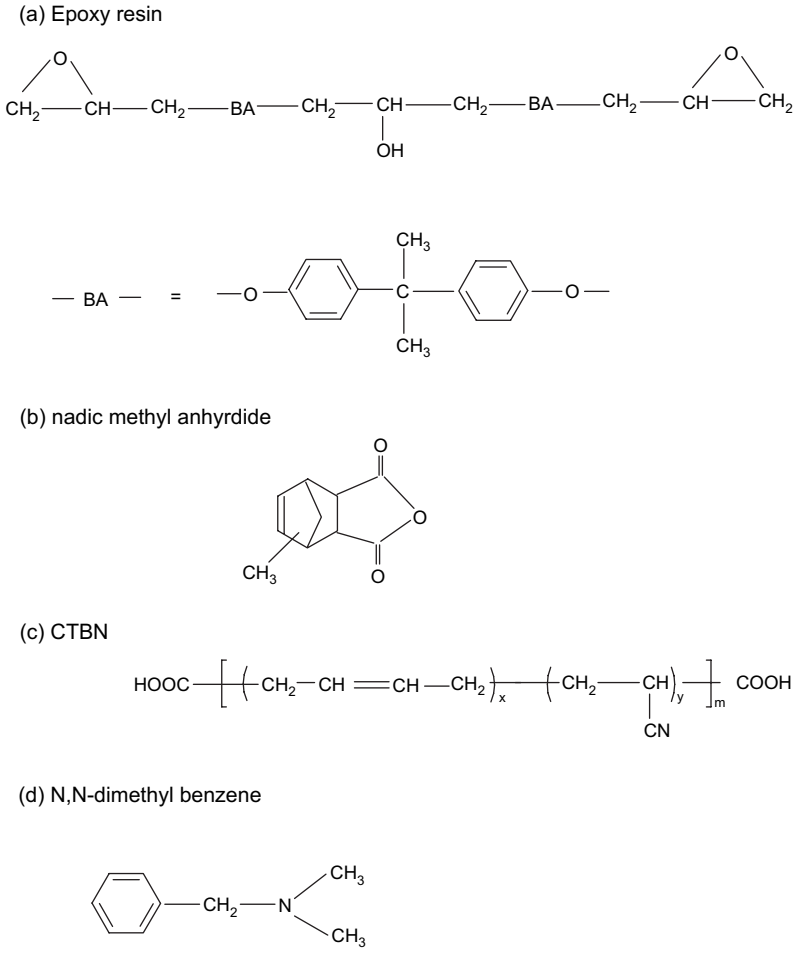

Fig. 1. Structure of compounds.

Table 1
Characteristics of CTBN

Properties[a]	CTBN (1300*8)
Molecular weight, M_n (g mol^{-1})	3500
Acrylonitrile content (wt%)	18
Viscosity, Brookfield, cp (300 K)	570,000
Specific gravity	0.960
Solubility parameter, δ (cal/cm^3)$^{1/2}$	9.14
T_g[b] (K)	215

[a] Material and data supplied by Huntsmann Co.
[b] Glass transition temperature determined by DSC.

2.3. Differential scanning calorimetry

The calorimetric measurements were performed with a Perkin–Elmer–Pyris DSC 6 differential scanning calorimeter supported by a Perkin–Elmer computer for data acquisition. The instrument was calibrated with indium and dry cyclohexane standards. Isothermal heating experiments were conducted in a nitrogen flow of 40 ml/min. The heating was done from room temperature to the temperature of the isotherm at a heating rate of 100 °C/min. Isothermal heating study was performed at three different curic temperatures: 120, 140, and 150 °C. The cure process and the thermal properties of the thermosetting material affect its macroscopic properties that mostly govern its end use applications and performance. Differential scanning calorimetric (DSC) analysis was employed to study the extent of the reaction. The analysis is based on the assumption that the heat generated during the epoxy curic reaction is equal to the total area under the heat flow–time curve. The degree of cure is then determined from the heat of reaction. The curic reaction was assumed to be complete when the isothermal curve of the blends leveled off to the base line. The areas of the peak under the isothermal curves at various times were used to determine the conversion (α) at various times. The conversion percentage was determined as

$$\alpha = \left(\frac{\Delta H_{\text{total}} - \Delta H_{\text{resid}}}{\Delta H_{\text{total epoxy}}}\right) \times 100 \quad (1)$$

The reaction rate, dα/dt has been calculated through the equation:

$$\frac{d\alpha}{dt} = \frac{(dH/dt)}{\Delta H_{\text{total epoxy}}} \quad (2)$$

where dH/dt is the heat flow as a function of the cure time obtained from the isothermal DSC experiments.

2.4. Phase-morphology studies

The samples were fractured under liquid nitrogen and the dispersed rubber phase was extracted using toluene for 10 h at ambient temperature. The dried samples were sputter-coated with gold prior to SEM examination. JEOL JSM 5800 model scanning electron microscope was used to view the specimens. Several micrographs were taken for each sample. The dimension of the dispersed phase was analyzed by image analyzer.

2.5. Dynamic mechanical thermal analysis

The viscoelastic properties of the modified epoxies as well as the neat resin cured at different temperatures were measured using TA instruments DMA 2960 dynamic mechanical thermal analyzer. The samples were cured at 140, 150, and 180 °C (as explained previously) and the analysis was done in a dual cantilever mode. The samples were heated from −100 to 250 °C at the heating rate of 3 °C/min. The frequency used was 1 Hz.

3. Results and discussions

Typical plots of conversion (α) versus time of the neat epoxy cured at various temperatures of study are shown in Fig. 2. The shape of the curve is similar to that expected for an autocatalytic reaction and similar to that observed for other epoxy matrixes [32]. The curing reaction of a thermoset is a thermally catalyzed one and maximum conversion is attained earlier at a higher curing temperature (T_{cure}). A similar trend was observed during the kinetic study of the curic reaction for a system of bisphenol-S epoxy resin (BPSER) with diaminodiphenyl sulfone (DDS) as a curing agent [33]. And also, the curic reaction kinetics of a system of *o*-cresol formaldehyde epoxy resin/succinic anhydride/tertiary amine, studied by Ma and Gao [25] have noted a similar thermal evolution. As the curing progresses, epoxy resin undergoes polymerization to form three-dimensional network and hence the T_g of the system increases. Complete cure usually occurs at temperatures in the vicinity of the maximum glass transition temperature. This is indicative of autocatalytic kinetics in the first stage of cure and diffusion controlled reaction (to be discussed later) as the T_g rises [33]. When $T_{\text{cure}} = 120$ °C, the conversion reaches only to a stage of $\alpha = 0.97$ and not to the maximum

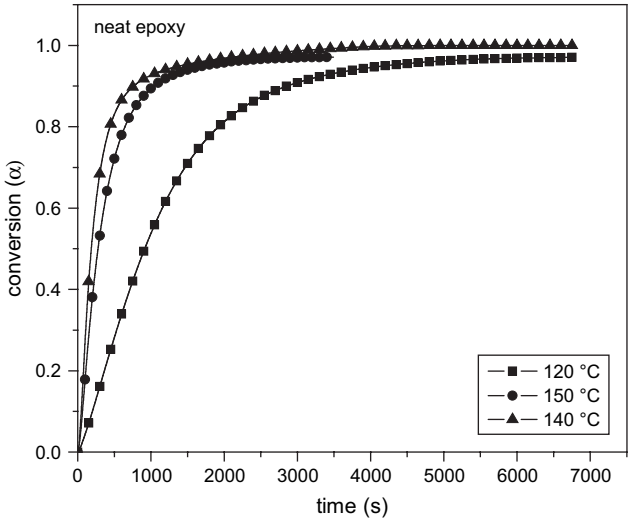

Fig. 2. Conversion versus time for neat epoxy cured at different temperatures.

level of $\alpha \approx 1.0$. Also, the maximum possible conversion occurs in a higher period of time ($t \approx 6740$ s). However, at a higher temperature ($T_{cure} = 140$ °C), the degree of conversion becomes maximum ($\alpha = 0.99$) in a lesser period of time. When $T_{cure} = 150$ °C, the conversion plot comes to an end at time $t \approx 3400$ s. Again it is interesting to notice a decrease in the maximum conversion by a fraction of 0.02 ($\alpha = 0.97$) when $T_{cure} = 150$ °C, as compared to that of a comparatively lesser curic temperature, $T_{cure} = 140$ °C ($\alpha = 0.99$). This can be explained based on the glass transition temperature of the neat epoxy matrix. The T_g of the cured neat epoxy when $T_{cure} = 140$ °C is 135 °C (as read from Fig. 14). It is nearer to the T_{cure} and maximum degree of conversion is possible at this temperature. However, when the sample gets cured at 150 °C, the reaction and hence the network formation becomes more speedy and the system reaches the stage of gelation before attaining the maximum degree of conversion. Also, in the present system, the initial speed of the reaction is slightly higher at 140 °C than at 150 °C. This may probably be attributed to the immediate incipient formation of cross-linking structures at high temperatures that causes to slow down the reaction comparatively.

Fig. 3 depicts conversion versus time at $T_{cure} = 150$ °C for neat and modified epoxies with varying weight contents of CTBN. At a particular cure time, there is slight reduction in conversion for rubber-modified systems which is mainly attributed to the physical changes like dilution effect and/or viscosity increase as a result of the liquid rubber addition [34–36] or by the reduction in the density of the reactive groups [37]. The thermoset reactions are accelerated by thermal effect. Similar final conversions after isothermal curing were observed by Fernandez et al. [38] for the tetraglycidyl diaminodiphenyl methane epoxy (TGDDM/DDM/PMMA) system.

Fig. 4(a)–(c) shows the isothermal rate of curing reaction versus time for the curing of the neat as well as CTBN-modified epoxies at 120, 140, and 150 °C, respectively. The

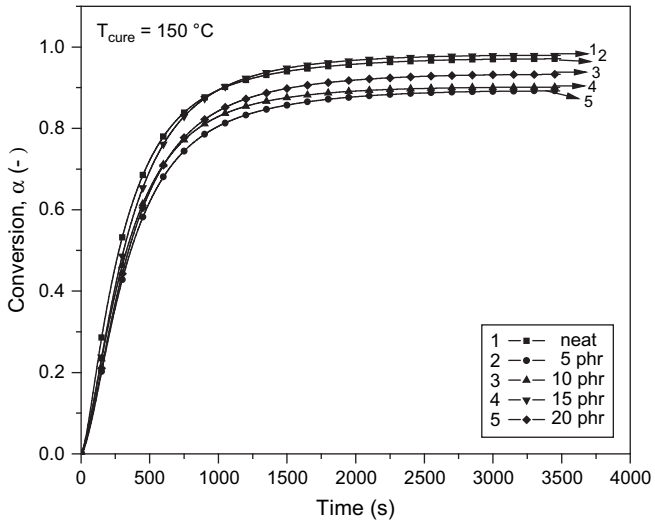

Fig. 3. Conversion versus time for neat and modified epoxies cured at 150 °C.

above curves illustrate that the rate of curing increases with increase in curic temperatures. The reaction rate increases with time at a particular temperature and it occurs through a maximum after the start of the reaction, showing autocatalytic nature. The reaction mechanism remained the same even after the inclusion of the liquid rubber. The maximum peak value of the rate of the reaction is higher as the isothermal temperature is higher and shifts to shorter period of time with increase in isothermal temperature.

It is significant to discuss the curic reaction mechanism of neat DGEBA/anhydride and DGEBA/anhydride/CTBN systems in this context. Scheme 1 explains the curic reaction mechanism between the anhydride and the epoxy resin. The reaction between the anhydride and the secondary hydroxyl group of the epoxy resin results in the formation of a monoester. The newly generated carboxyl group, then, reacts with the epoxide group and also with the secondary hydroxyl group to form a diester. Thus the curic reaction initiates to form a network structure.

It is a known fact that the interaction of epoxy compounds with anhydrides, amines and other nucleophiles is promoted by the addition of hydroxyl-containing compounds like water, alcohols, phenols, etc. Here the reaction is supposed to proceed, initially, through a trimolecular transition state as Smith [39] has explained in the reaction of epoxy compounds with amines as shown below:

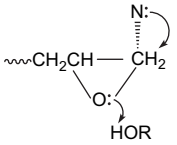

The reaction was found to obey an *n*th order kinetics (to be discussed later) as the maximum curic reaction rate was observed at $t = 0$ when carried out in the presence of hydroxyl-containing solvent. This is due to the participation of proton. But the cure kinetics of neat as well as modified epoxies show a maximum reaction rate at $t > 0$, negating the simple *n*th order kinetics.

Also, the tertiary amine acts as a catalyst during the course of the reaction and the reaction is initiated by the activation of the anhydride as illustrated in Scheme 2. The negative oxygen ion reacts with the epoxy group as well as with the anhydride. The mechanism is not a typical tertiary amine catalytic reaction, as the amine is not reformed in the reaction. Thus, an excellent network structure is formed in the epoxy–anhydride system [40]. As curing progresses, the cross-linking density of the matrix increases and the liquid rubber became no more soluble in the epoxy and ultimately the rubber gets phase separated out as domains in the epoxy matrix. These domains hinder the curing reaction and the system reaches to a vitrified state – a physical transformation from liquid to glassy state via rubbery state.

Typical plots of the rate of cure versus conversion for the neat and modified systems at 120, 140, and 150 °C curic temperatures are depicted in Fig. 5(a)–(c). From the figures it is evident that the reaction rate for higher modified systems and the extent of conversion for all modified systems

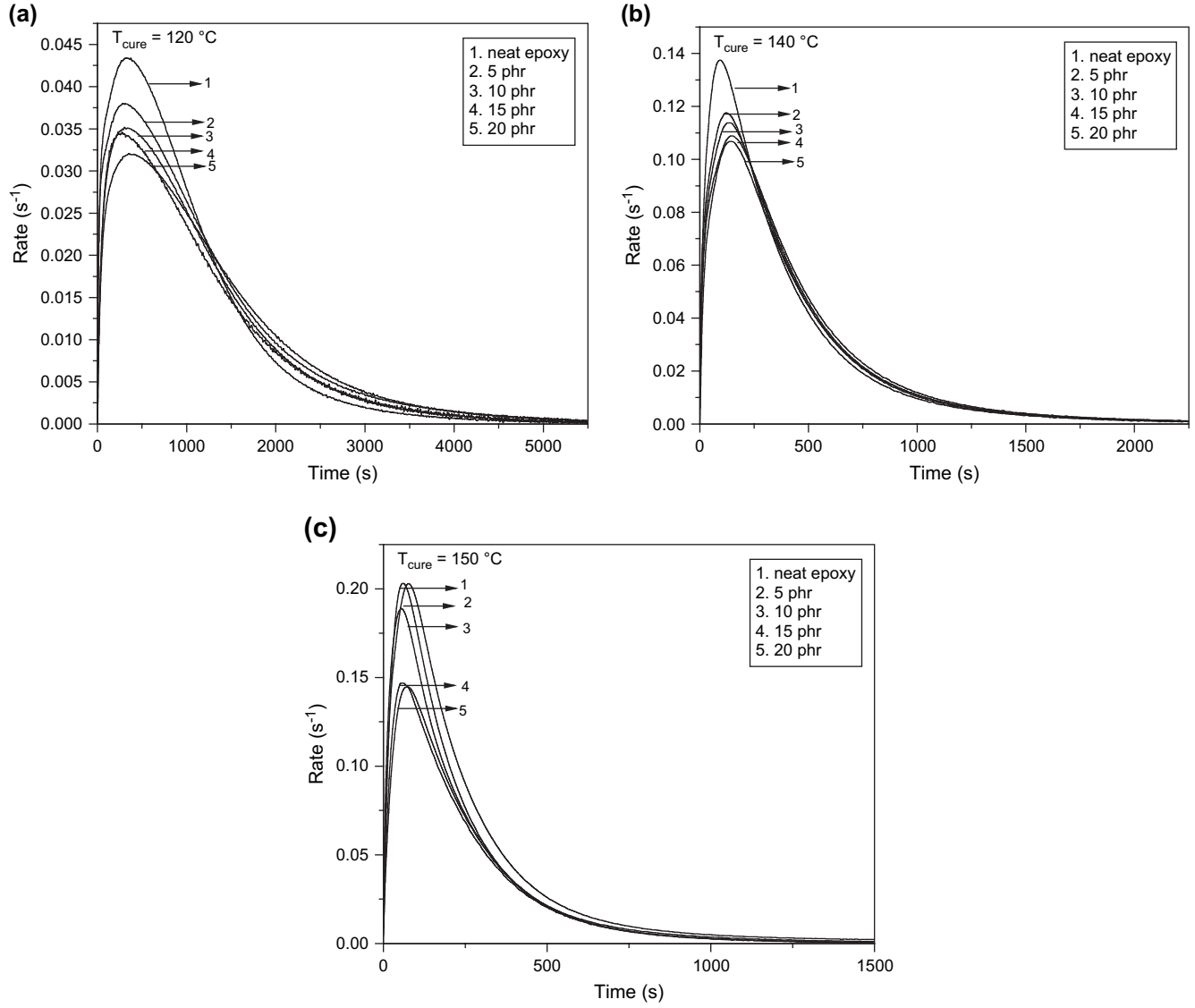

Fig. 4. Rate versus time for neat and modified epoxies at an isothermal curic temperature of (a) 120, (b) 140, and (c) 150 °C.

decreased with increase in CTBN content at a particular temperature. The rate of conversion significantly increases with increase in temperature for neat as well as modified systems, showing the thermal effect of the curic reaction. A linear enhancement in the reaction rate with conversion was indicated for all modified systems during the initial stages of cure at all temperatures. However, a deviation in the rate of reaction from linearity was noticed as conversion proceeds (up to 60–80% of conversion, depending on the curing temperature). Deviations observed are attributed to the fact that the reaction becomes diffusion controlled at the onset of gelation (the diffusion controlled model to be discussed next). As the curic reaction proceeds, the epoxy resin seems to develop a three-dimensional network structure with the liquid rubber, as the carboxyl functionality of the CTBN and hydroxyl functionality of the epoxy resin react to a certain extent. The course of the reaction is depicted in Scheme 3. The carboxyl functionality of CTBN reacts with the secondary hydroxyl groups of the epoxy resin to form a diester. Similarly, the carboxyl groups can also react with the epoxide group to generate a diester. Thus, a large excess of bisepoxy resin results and the rubber being encapped at both ends by one unit of epoxy. Further reaction of the rubber containing diepoxide may occur with the unreacted epoxy. The overall contribution of Schemes 1–3 results in the formation of a three-dimensionally cross-linked network. There is a simultaneous increase in molecular weight and viscosity along with the development of the network structure. As a result, the rubber and epoxy become less compatible and a phase separation state is reached whereby rubber-rich domains precipitate in the epoxy-rich matrix and the liquid rubber becomes phase separated. Thus ultimately, in the late stage of the curing process, the sample approaches a solid state. The movement of the reacting groups and the products is greatly diminished and the rate of reaction, which was previously controlled by the chemical kinetics, now becomes diffusion controlled. Now the movement of the reacting groups and the products is possible only by diffusion. Thus the curing slows down since further possible reaction is only due to

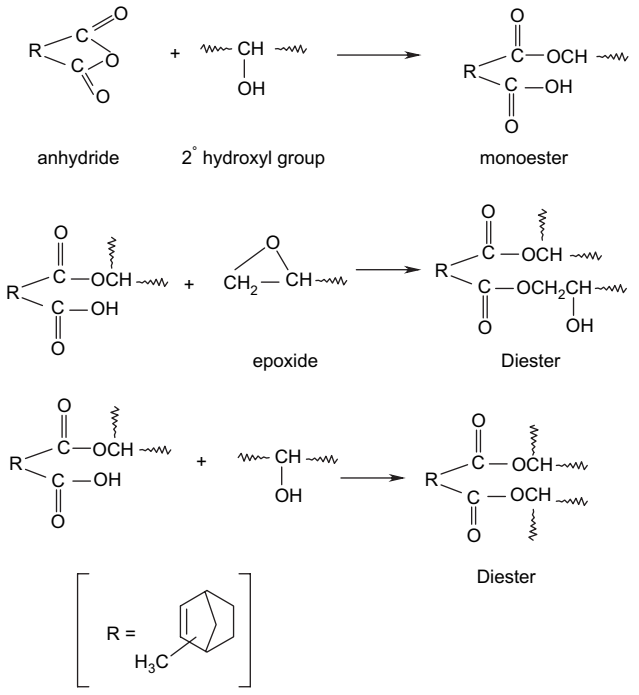

Scheme 1. Curic reaction mechanism of the anhydride and the epoxy resin.

diffusion. Higher rubber content inclusion may cause more dilution and thus flexibilize the matrix instead of enhancing the reaction rate.

3.1. Kinetic model and activation energies

Many researchers [41–43] have employed an *n*th order kinetic model to explain the curic reactions of a thermoset. But the defect of these models is the lack of prediction of the peak observed in the isothermal rate of the reaction curve or the sigmoidal shape of the heat of the reaction curve. Also such a kinetic model could never explain the entire curic reaction of a thermoset due to the physical transformations such as gelation and vitrification occurring during the curic reaction that lead to the network formation of the matrix. It is evident from the curves that a maximum reaction rates are attained at time $t > 0$, and hence the *n*th order kinetics becomes invalid and suggests the autocatalytic model. The *n*th order kinetic model is applicable only if the maximum reaction rate is observed at $t = 0$. But as per the autocatalytic model, the rate attains a maximum value at an intermediate conversion. The autocatalytic kinetics, expressed by Kamal [44], as given below, is suitable to explain the isothermal curing behavior.

$$\frac{d\alpha}{dt} = (k_1 + k_2\alpha^m)(1-\alpha)^n \tag{3}$$

where α = extent of the reaction, obtained by the partial area under a DSC trace versus time, t. k_1 and k_2 are the specific rate constants of the models and are functions of temperature, m and n are the reaction orders and $(m+n)$ is the overall reaction order. Eq. (3) represents the experimental observations (Fig. 4(a)–(c)) that the maximum in the exothermal curve occurs at some point $t > 0$, and that the rate of the reaction at $t = 0$ is not zero, thereby excluding the simple *n*th order kinetics. This has been successfully applied to similar epoxy systems [18]. To compute the parameters of Eq. (3) from experimental data, several methods have been proposed in the literature [45–48]. In many of them the total reaction order $(m+n)$ was assumed to be 2, restraining the range of application of the proposed model.

To investigate the cure kinetics, isothermal DSC scans were done at three curing temperatures say at 120, 140, and 150 °C. The experimental value of the rate of reaction $d\alpha/dt$ and conversion (α) for the complete course of the reaction was computed and adjusted with the kinetic equation. In the present study, the kinetic parameters k_1, k_2, m and n were estimated without any constraints on them by fitting the experimental data of $d\alpha/dt$ versus α at different temperatures using a non-linear least-square procedure. The typical representative plots of the experimental data and the data obtained by autocatalytic model for the neat as well as modified epoxies at curic temperatures 120 and 140 °C are shown in Figs. 6 (a–e) and 7 (a–e). The data of experimental as well as model predictions are well in agreement at lower conversions, which represent the initial

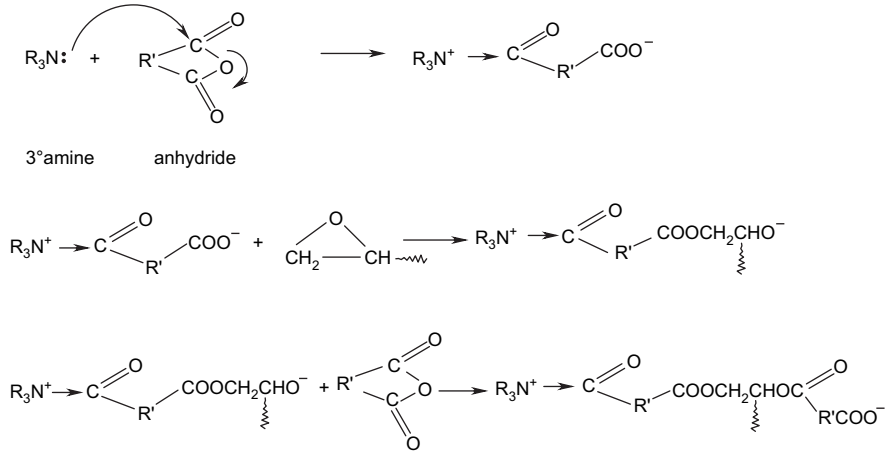

Scheme 2. Curic reaction mechanism of the anhydride and the epoxy in the presence of a tertiary amine.

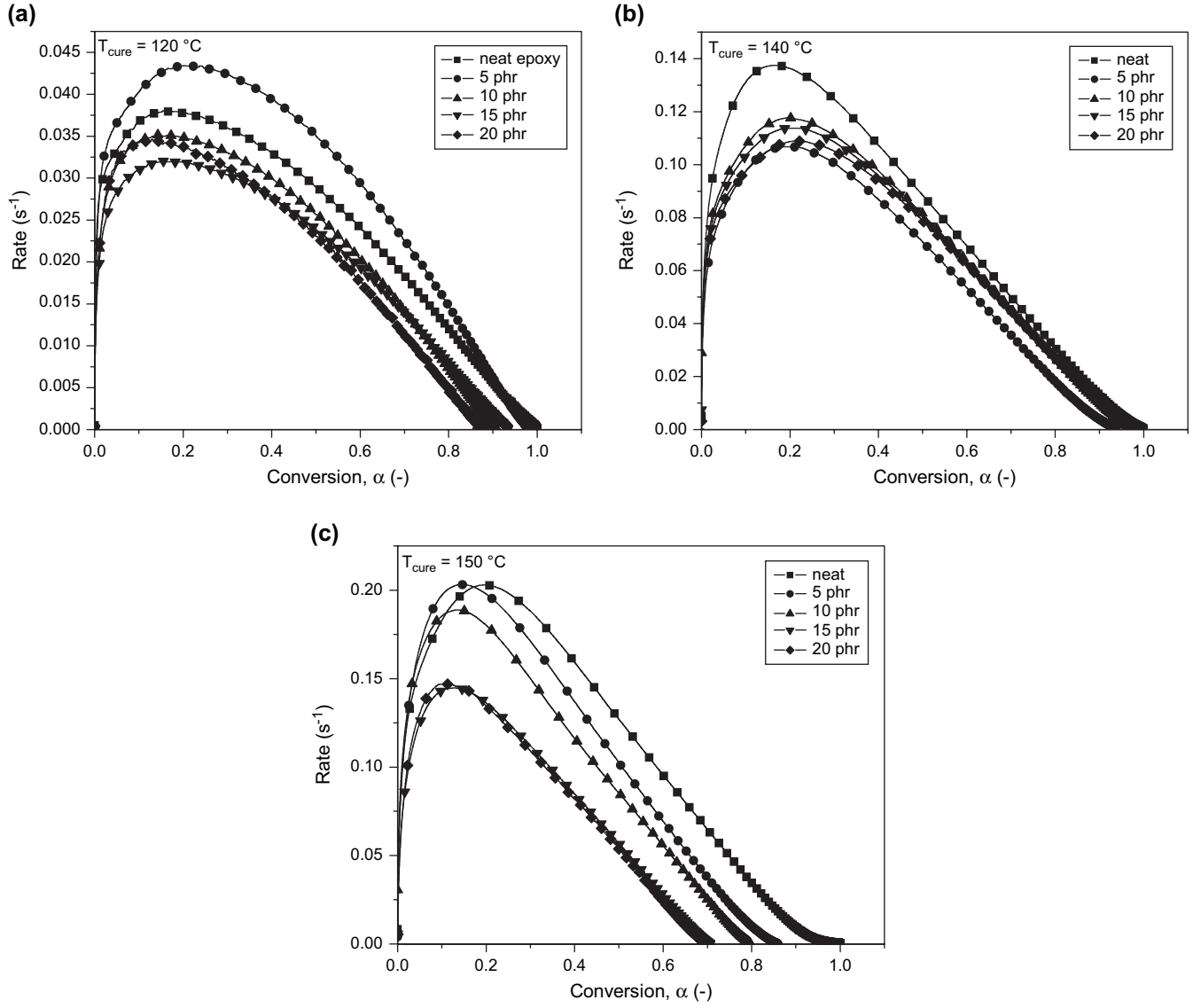

Fig. 5. Rate versus conversion for neat and modified epoxies at an isothermal curic temperature of (a) 120, (b) 140, and (c) 150 °C.

stages of the curic reaction. But in the later stages of the curic reaction, i.e., at higher conversions the data of the model predictions slightly deviate from that of the experimental. Thus in the later stages of cure, the reaction was controlled by diffusion mechanism rather than by kinetic parameters. Difference between model predictions and experimental data is observed

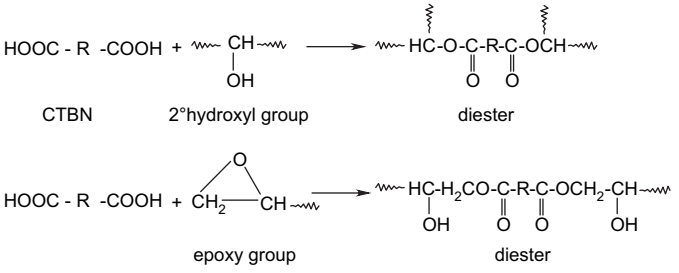

Scheme 3. Curic reaction of CTBN with epoxy resin.

to be greater when curing temperature decreases. This is related to the T_g of the fully cured material. The free volume is reduced, if the curing temperature is close to the glass transition region of the highly cured material. The segmental mobility within the polymer decreases, thereby reducing the rate of diffusion of the molecules to the reactive sites. Thus the reaction rate decreases. Since there are two kinetic constants k_1 and k_2, two activation energies Ea_1 and Ea_2 could be obtained by plotting $\ln k_1$ and $\ln k_2$ versus $1/T$. The slopes of the plots were used to estimate the activation energies Ea_1 and Ea_2. The kinetic parameters obtained for the systems at all curic temperatures after a large number of iteration are given in Tables 2–4. The overall reaction order $(m+n)$ was observed to be in the range of 1.5–2.5 at 120 and 140 °C and greater than 2 at 150 °C. The values of m and n were in the range of 0.5–1.0 and 1–2.5 for the neat resin as well as for the blends. Generally speaking, the $(m+n)$ value increases with temperature. This is attributed to the trimolecular

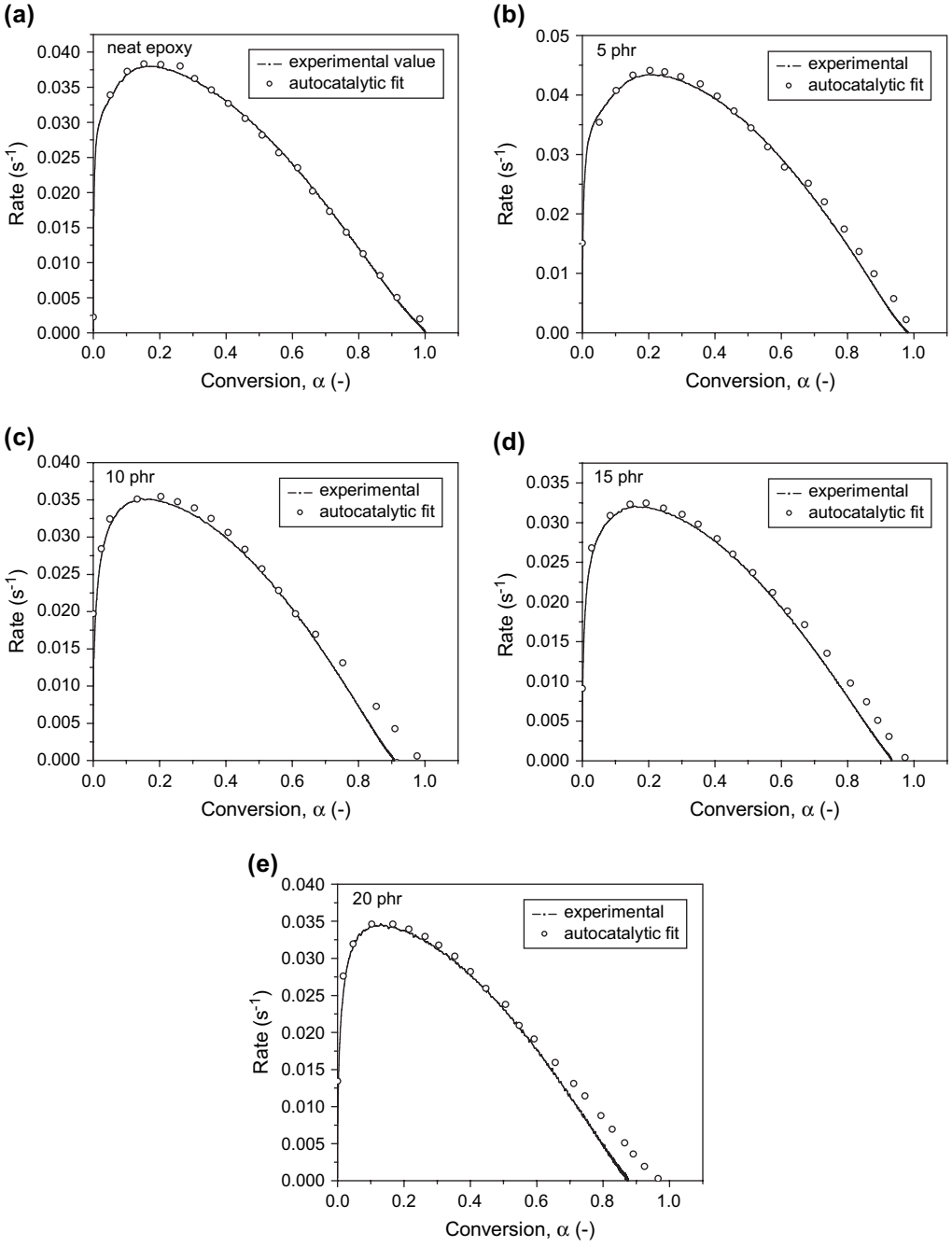

Fig. 6. (a–e) Comparison of experimental data with model predictions: rate versus conversion at 120 °C.

mechanism reported earlier [39]. Few of the hydroxyl groups in the molecular chain of the epoxy resin participate in the reaction. However, this curing reaction is not a standard *n*th order reaction. The −OH group in the molecular chain of the epoxy resin can become proton donor and participate in the reaction with the increasing curing temperature. The reaction should follow a trimolecular mechanism with the participation of the proton. This is the reason for the increase in the $(m+n)$ value with the temperature. Similar results in the curing of epoxies are reported elsewhere [25]. The correlation for k_1 values was found to be poor compared with that for k_2. This is because k_1 is computed only with the two or three of the first experimental data that may lead to imprecise calculated values. It was observed that generally the k_1 values of neat and modified epoxies are low compared with those obtained for k_2. According to Arrhenius relationship, the reaction constants k_1 and k_2 depend on temperature, as per the relation:

$$k = A\exp(-E_a/RT) \tag{4}$$

The higher values of the reaction rates are evident in this system. Fig. 8 is a typical Arrhenius plot. The activation energy values, Ea_1 and Ea_2, obtained for the neat epoxy and CTBN-modified epoxies are tabulated in Table 5. The activation

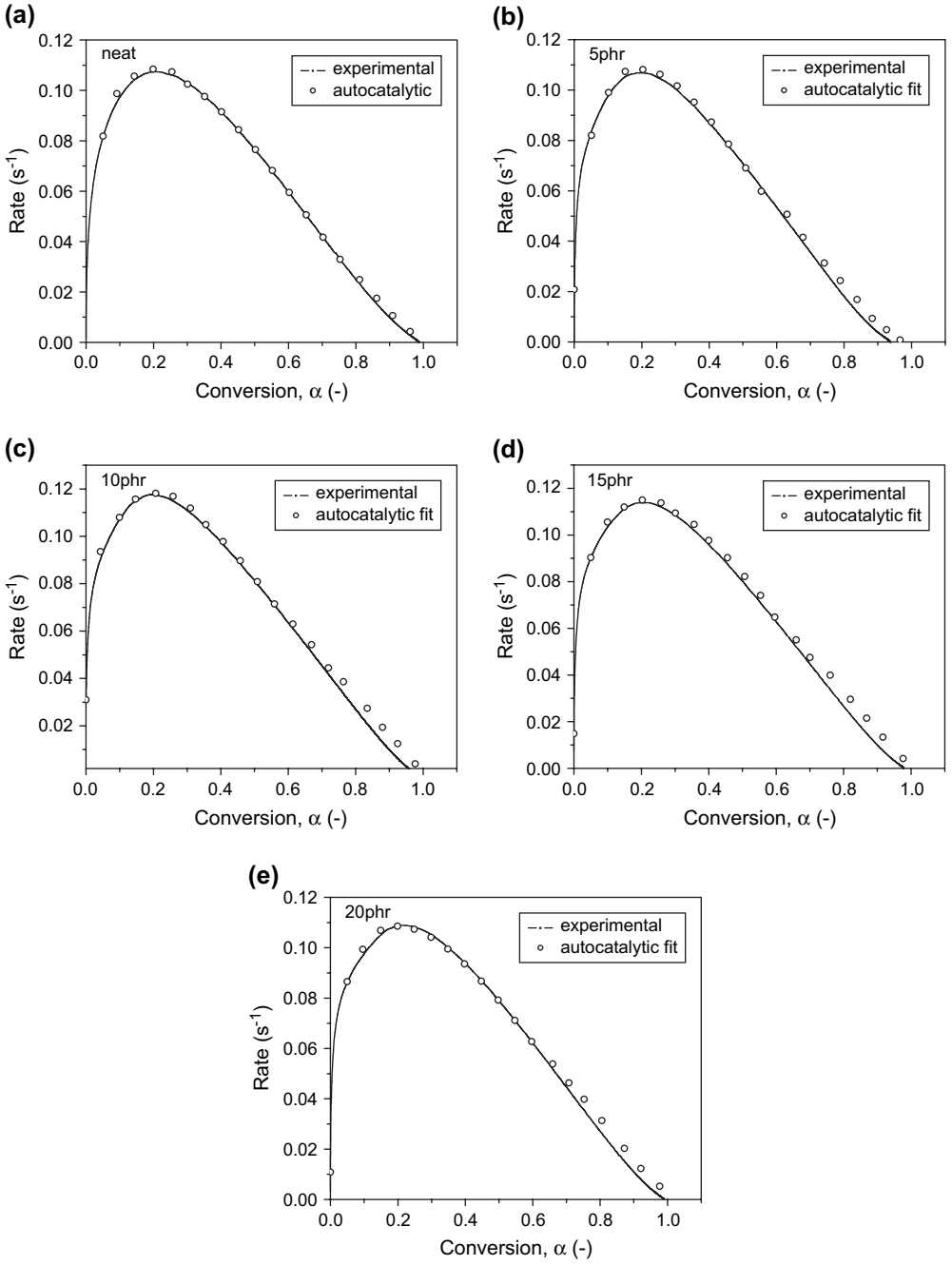

Fig. 7. (a–e) Comparison of experimental data with model predictions: rate versus conversion at 140 °C.

energies for the curing of CTBN-modified blends exhibit a larger value compared to the neat resin. This is because the phase separated CTBN hinders the reaction between epoxide and anhydride.

3.2. Diffusion factor

The diffusion control in curic reaction was explained by a semiempirical relationship. This is based on free volume

Table 2
Autocatalytic model constants for CTBN-modified epoxy blends at 120 °C

Epoxy systems	m	n	$m+n$	$k_1 \times 10^{-3}$ (min^{-1})	$k_2 \times 10^{-3}$ (min^{-1})
Neat epoxy	0.23	1.05	1.28	2.2	67.1
5 phr CTBN	0.47	1.22	1.69	15.0	91.8
10 phr CTBN	0.88	1.07	1.95	25.3	93.6
15 phr CTBN	0.47	1.51	1.98	33.8	92.0
20 phr CTBN	0.61	2.01	2.62	13.4	115.3

Table 3
Autocatalytic model constants for CTBN-modified epoxy blends at 140 °C

Epoxy systems	m	n	$m+n$	$k_1 \times 10^{-3}$ (min^{-1})	$k_2 \times 10^{-3}$ (min^{-1})
Neat epoxy	0.24	1.33	1.57	15.8	291.0
5 phr CTBN	0.52	1.81	2.33	20.8	325.0
10 phr CTBN	0.45	1.47	1.92	31.1	270
15 phr CTBN	0.39	1.43	1.82	14.8	264
20 phr CTBN	0.36	1.34	1.70	11.0	243

Table 4
Autocatalytic model constants for CTBN-modified epoxy blends at 150 °C

Epoxy systems	m	n	$m+n$	$k_1 \times 10^{-3}$ (min^{-1})	$k_2 \times 10^{-3}$ (min^{-1})
Neat epoxy	0.40	1.69	2.09	23.6	539
5 phr CTBN	0.68	2.89	3.57	50.6	1167
10 phr CTBN	1.02	2.70	3.72	89.0	1852
15 phr CTBN	1.3	2.5	3.8	64.8	3836
20 phr CTBN	1.5	2.6	4.1	75.4	460

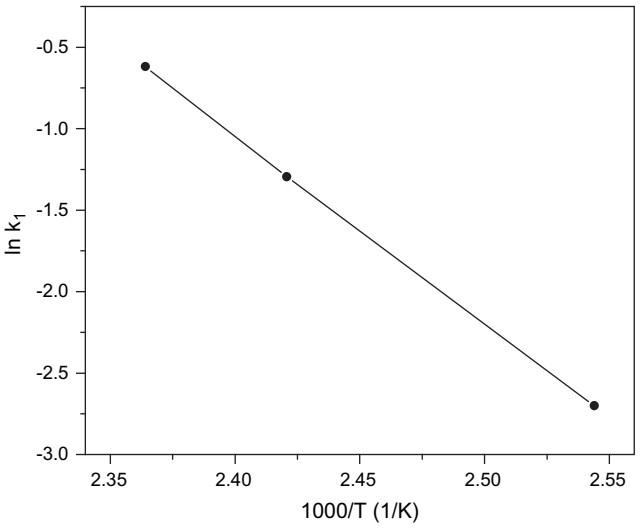

Fig. 8. Arrhenius plot for rate constants.

considerations and was proposed by Chern and Poehlein [49], Khana and Chanda [50] have successfully applied this equation for a catalyzed epoxy–anhydride system. After attaining a critical value, α_c, the conversions become diffusion controlled and the corresponding rate constant, k_d, is given by:

$$k_d = k_c e^{(-C(\alpha-\alpha_c))} \tag{5}$$

where k_c is the rate constant for chemical kinetics and C is a parameter.

Eq. (5) means an abrupt change in the diffusion control from chemical control for the curic reaction after the conversion reaches the critical value, α_c. But this change is gradual and there is a region where both factors control.

The overall effective rate constant, k_e, can be expressed in terms of k_d and k_c.

$$\frac{1}{k_e} = \frac{1}{k_d} + \frac{1}{k_c} \tag{6}$$

Table 5
Activation energy values for neat and modified epoxies

Epoxy systems	Ea_1 (kJ mol^{-1})	Ea_2 (kJ mol^{-1})
Neat epoxy	71.2	96
5 phr CTBN	73.1	112.2
10 phr CTBN	75.4	118.6
15 phr CTBN	81.5	122.4
20 phr CTBN	98.4	140.3

The diffusion factor, $f(\alpha)$ [51], is defined from the above equations as:

$$f(\alpha) = \frac{k_e}{k_c} = \frac{1}{1 + e^{(-C(\alpha-\alpha_c))}} \tag{7}$$

with C and α_c, the diffusion coefficient and the critical conversion, being two empirical parameters. When α is much smaller than the critical value, $\alpha \ll \alpha_c$, $e^{(-C(\alpha-\alpha_c))} \approx 0$, then $k_e \approx k_c$, $f(\alpha)$ approximates to unity, the reaction is kinetically controlled and the effect of diffusion is negligible. When α increases and approaches to α_c, $f(x)$ begins to decrease. At $\alpha = \alpha_c$, $f(x)$ becomes 0.5 and beyond this point, approaches zero as the reaction effectively stops. But the change is not abrupt, rather a gradual one. This is the region where both factors are controlling. The effective reaction rate at any conversion is given by the chemical reaction rate multiplied by $f(\alpha)$ [22].

The value of $f(\alpha)$ is considered as the ratio of the experimental reaction rate to the reaction rate predicted by the autocatalytic model. During the early stages of cure the value of $f(\alpha)$ is near unity. As the curing proceeds, the value decreases due to the onset of diffusion control. Fig. 9 depicts the plots of $f(\alpha)$ versus conversion, α, at different curing temperatures for a 10 phr modified system. A possible explanation can be given on the basis of the change in the T_g values as curing progresses. A schematic model of the curic reaction and the resulting phase separation phenomenon is illustrated in Fig. 10. At the initial stage, a homogenous blend was obtained as represented in A, which consists of only the components of the blend. The short wavy lines represent the components of the blend. At the very start of the curing reaction the degree of cure was low and the system had a very low T_g value. As the reaction proceeds, a gradual and slow increase in molecular weight takes place and this transition is a reflection of the movement of linear molecular chains that are formed in the system, represented by B. During this early stage of

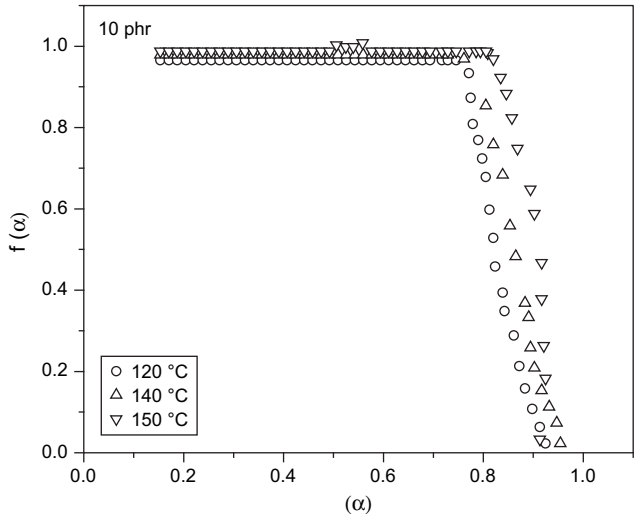

Fig. 9. Plot of diffusion factor, $f(\alpha)$, versus conversion at different curic temperatures for 10 phr modified epoxy.

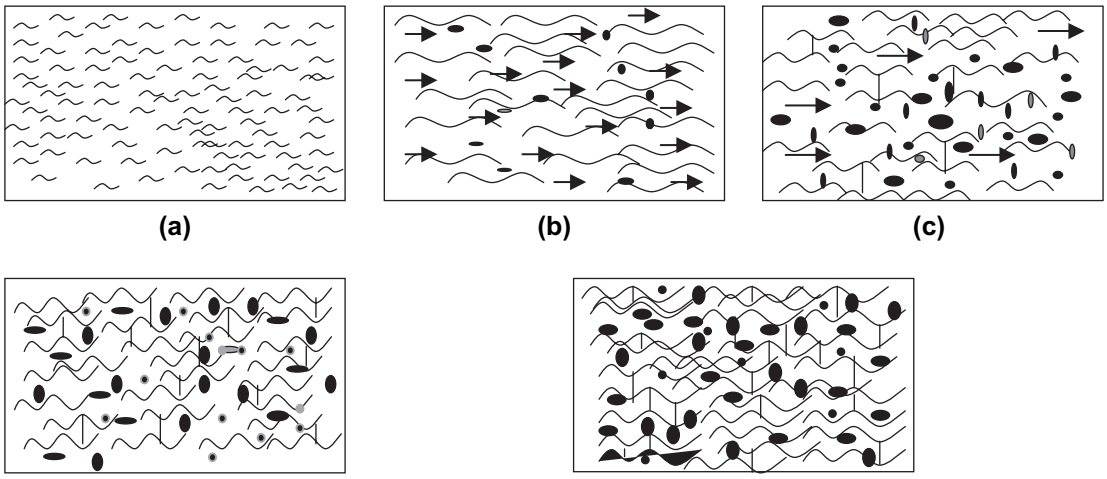

Fig. 10. A schematic representation of curic reaction and phase separation.

polymerization, only linear molecular chains prevailed in the system and have enough freedom to collide with other molecules to participate in the reaction. The long wavy lines represent linear chains. This resulted in a high reaction rate. A number of arrows symbolize this situation. Phase separation initiates at this stage, shown by spherical domains. As the molecular weight is further increased, the system attains a gel state, the mobility was limited, and reaction rate decreased and became diffusion controlled. The reduction in the number of arrows and later the broken arrows signifies this transformation. Few cross-links are also developed during this change of state. The phase separation and the formation of domains become maximum. Both C and D in the scheme represent this stage of development. The cross-linking density increased with cure time, and the T_g of the network was increased with a reduction in the distance between cross-link points. The T_g value, further, increased and approached T_{cure}, the sample attained the vitrified state as represented by E.

4. Morphological analysis

Scanning electron microscopy (SEM) was used to examine the cryogenically fractured surface of the neat and rubber-modified epoxies to reveal the texture and morphology of the phase separated system. The glassy fracture surface in the SEM photograph (Fig. 11) of the neat resin cured at 150 °C shows ripples that are due to the brittle fracture. The initial transparency of the blend of the neat epoxy sample indicates a high degree of miscibility between DGEBA and the hardener. The fractured surface of all modified epoxies showed a two-phase morphology with a rigid continuous phase and a dispersed rubbery phase of isolated spherical particles. The micrographs of the CTBN-modified epoxies (5–20 phr) cured at 140, and 150 °C are shown in Figs. 12 (a–d) and 13 (a–d), respectively. During the early stages of cure, the soft elastomeric phase is separated from the hard epoxy matrix. However, the epoxy phase contains a certain amount of dissolved rubber phase. As the concentration of CTBN was increased, the domain size increased. This follows a similar pattern to other epoxy–rubber blends [52]. Initially CTBN was miscible with epoxy resin and as the curic reaction proceeded the molecular weight of the system increased and a situation was reached where CTBN got phase separated from the epoxy at the onset of gelation process – a reaction induced phase separated system. A single phased homogenous system, thus, transformed into a phase separated gel state and finally to the glassy vitrified state, near T_{cure}. The segregation of the elastomeric phase is prominent at higher concentration of rubber phase and hence it was the reason for the comparatively large particle size in higher liquid rubber-modified epoxies. The morphological analysis for the samples cured at 140 and 150 °C have been quantified to find the number average (D_n), volume average (D_v) and weight average (D_w) of domain sizes and to compute the polydispersity index. The results are tabulated in Table 6. The number average, weight average, and the volume average of the dispersed domains decreased with increasing temperature. As curing temperature (T_{cure}) decreased particle size increased. At high curing temperature, the rate of epoxy curic reaction is high. The onset of gelation was attained at a lesser time (DSC measurements confirm this),

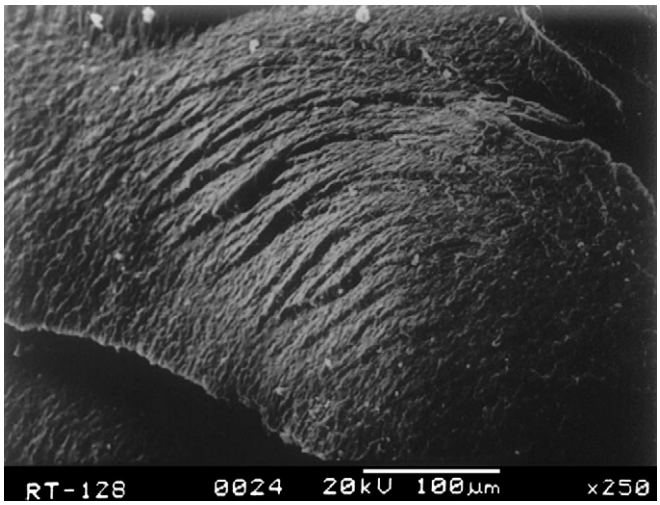

Fig. 11. SEM micrographs of the neat resin cured at 150 °C.

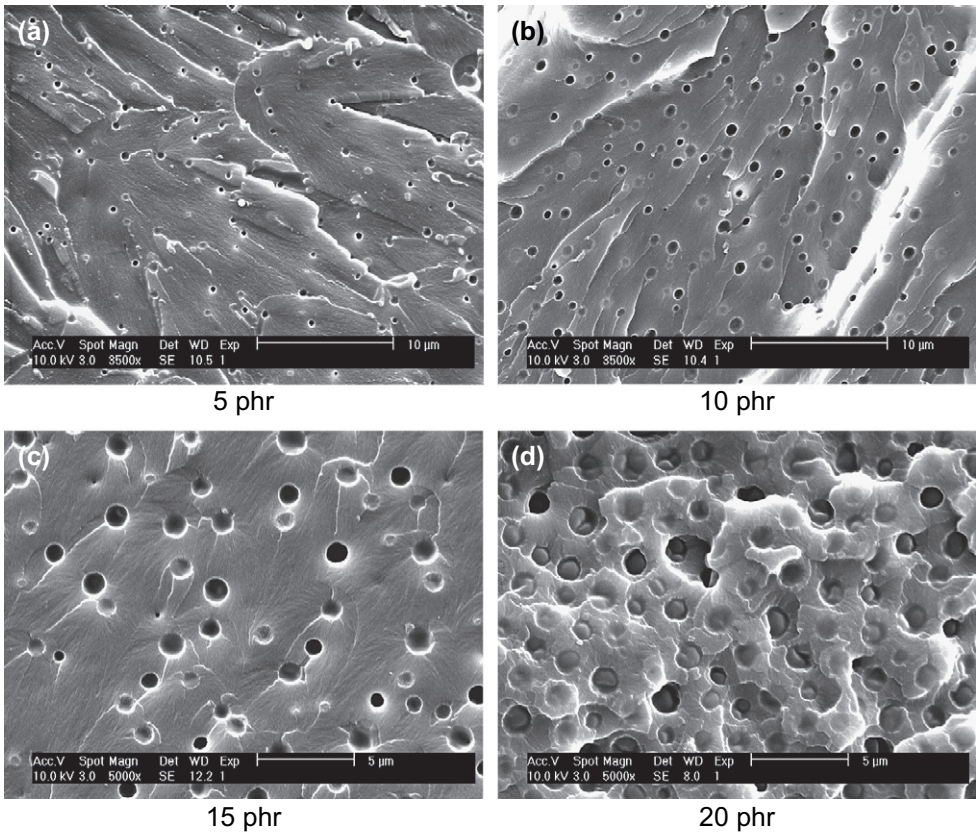

Fig. 12. SEM micrographs of the modified blends cured at 140 °C.

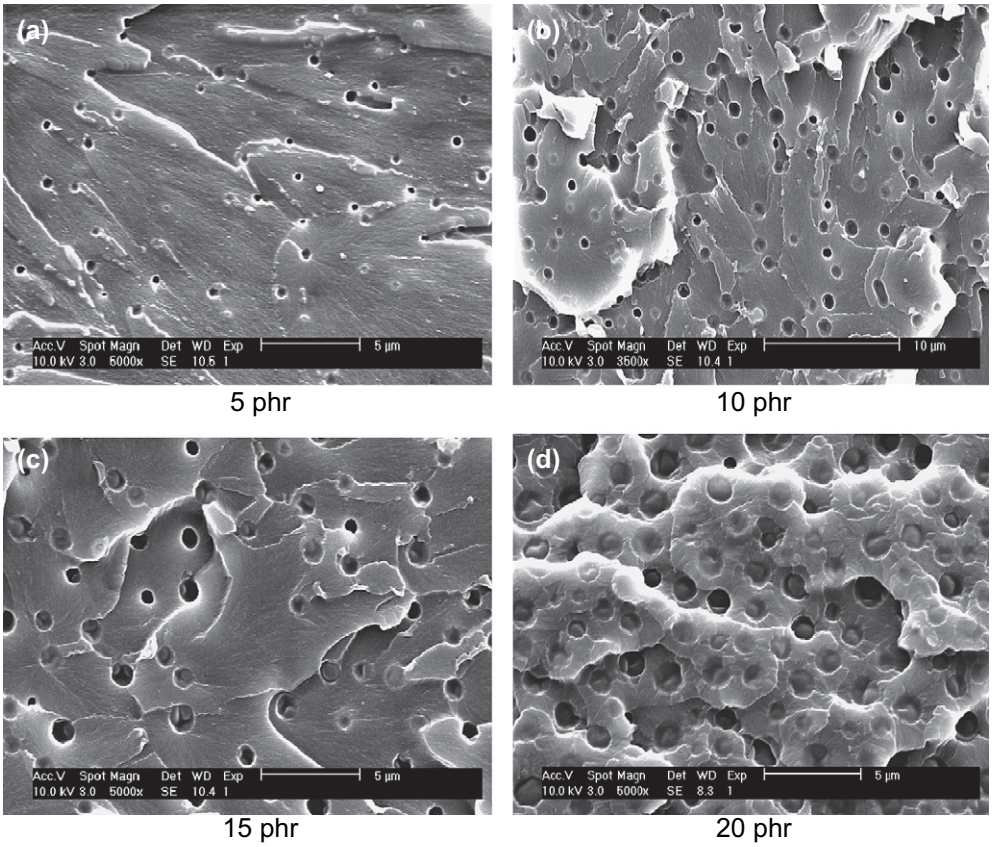

Fig. 13. SEM micrographs of the modified blends cured at 150 °C.

Table 6
Dispersed particle size and polydispersity of the modified epoxies cured at different temperatures

CTBN composition (phr)	Curing temperature (°C)							
	140				150			
	D_n (μm)	D_v (μm)	D_w (μm)	PI	Dn (μm)	D_v (μm)	D_w (μm)	PI
5	0.84	1.31	0.90	1.07	0.81	1.28	0.87	1.06
10	0.86	1.42	0.93	1.08	0.82	1.39	0.92	1.11
15	0.87	1.53	0.97	1.11	0.86	1.46	0.94	1.09
20	0.91	1.65	1.05	1.15	0.88	1.55	0.97	1.10

which resulted in a lower degree of coalescence of particles and ultimately in the phase separation of smaller particles. The increase in the viscosity of the system, the difference in the solubility parameters, and surface tension of the rubbery phase [53] during the cure process, all adds to the formation of particles. The volume average domain size increased with the concentration of CTBN content at a particular temperature. The polydispersity index was found to be greater than one in all cases.

5. Dynamic mechanical thermal analysis (DMTA)

Fig. 14 represents tan δ versus temperature plots for the neat epoxy resin cured at 140, 150, and 180 °C. T_g decreases with decrease in curing temperature. The decrease in T_g was attributed to the reduced conversion as a result of the lowering of curing temperature. The reaction practically stops after attaining the vitrified state.

The tan δ versus temperature curves for neat and modified epoxies at $T_{cure} = 180$ °C with different wt% of CTBN are shown in Fig. 15(a). The low-temperature region of the above relaxation curves is depicted in Fig. 15(b). The modified epoxies show two relaxation peaks. The higher peak noted at ca.140 °C is the T_g of the cured sample. The peak observed

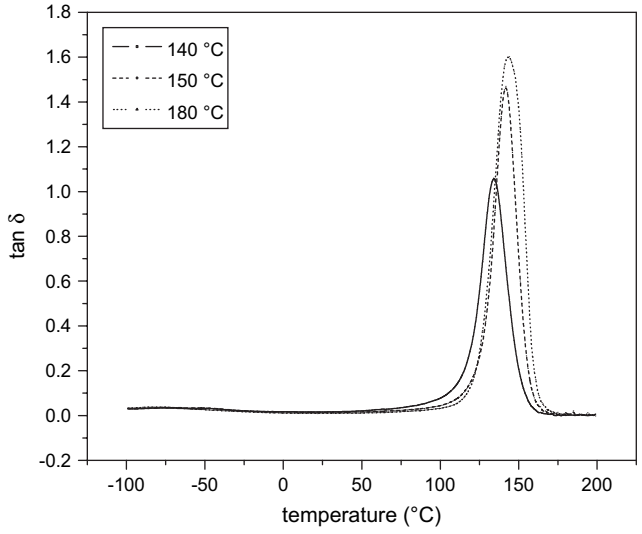

Fig. 14. Tan δ versus temperature of the neat epoxy cured at 140, 150, and 180 °C.

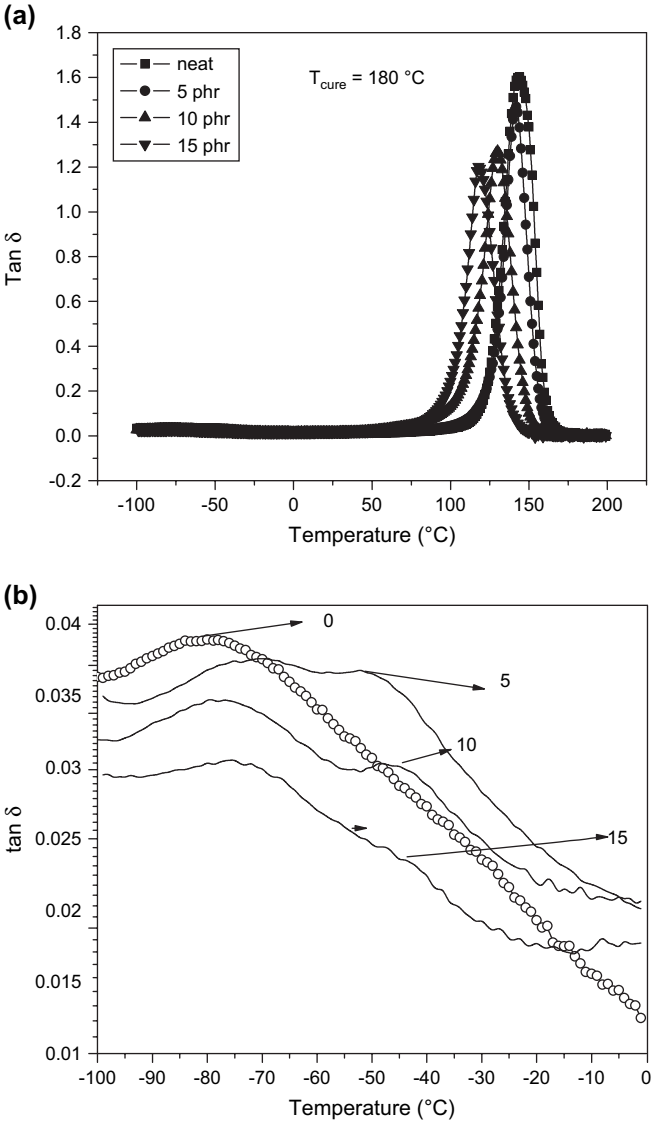

Fig. 15. (a) Tan δ versus temperature of the neat and modified epoxies at $T_{cure} = 180$ °C. (b) Low-temperature region of the curves showed in (a).

at ca. −50 °C, β transition, is assigned due to the glass transition of rubber as reported in the literature [54]. The addition of the liquid rubber lowers the T_g of the cured network, however, this become more significant when the wt% of CTBN is higher. This is due to the incorporation of the liquid rubber phase into the epoxy matrix where it acts as a flexibilizer. The pure epoxy also shows a broad peak at low temperature and this is contributed due to the crankshaft motion of the glyceryl-like groups in DGEBA [55,56]. The CTBN addition resulted in a slight change in the β-transition temperature. As the weight content of rubber increased, the T_g of the rubber moved slightly to higher temperature. This shows that the rubber domains have epoxy dissolved within the system in a molecular scale. Similarly, the continuous epoxy phase has some dissolved rubber phase which is miscible in a molecular scale. T_gs of the neat and various wt% modified blends at different T_{cure}s are tabulated in the Table 7. The T_gs of both phases decreased with decrease in curing temperature. A

Table 7
T_g of CTBN-rich and epoxy-rich phases of blends cured at different temperatures

CTBN composition (phr)	Curing temperature (°C)					
	180		150		140	
	Epoxy rich	CTBN rich	Epoxy rich	CTBN rich	Epoxy rich	CTBN rich
0	143.9	–	141	–	133	–
5	140.6	−68	138	−69	130	–
10	132.8	−48	129.5	−52.5	127.2	−53.2
15	123.0	−43	121.2	−45	120.0	−46
100	–	−78	–	−79	–	−80

schematic representation of the modified blend is depicted in Fig. 16, which illustrates both of these phases in a modified blend.

The storage modulus of neat resin and the modified epoxies with 5−20 wt% of CTBN are depicted in Fig. 17(a). The storage moduli of the modified epoxies with lower content of CTBN are greater while that of a 20 phr blend is lower than that of the neat resin. At lower concentration, the phase separated CTBN leads to improved fracture toughness of the epoxy network. At a higher concentration, the liquid rubber flexibilizes the epoxy matrix and reduces the cross-linking density. The decrease in the storage modulus is attributed to the lowering of the cross-linking density and plasticization effect of the liquid rubber into the epoxy matrix.

Fig. 17(b) represents the loss modulus, E'' versus temperature for neat and modified blends at $T_{cure} = 140$ °C. The transition peak becomes more intense by the cross-linking. With more and more inclusion of rubber, the peak shifts to lower temperature. This is attributed to the dissolution of rubber into the epoxy network, forming homogenous epoxy-rich phase. Another reason for the peak shifting and broadening could be the decrease in the cross-linking density of the epoxy upon the incorporation of rubber. The distribution of relaxation times of molecules in the epoxy matrix becomes broader by the inclusion of more rubber.

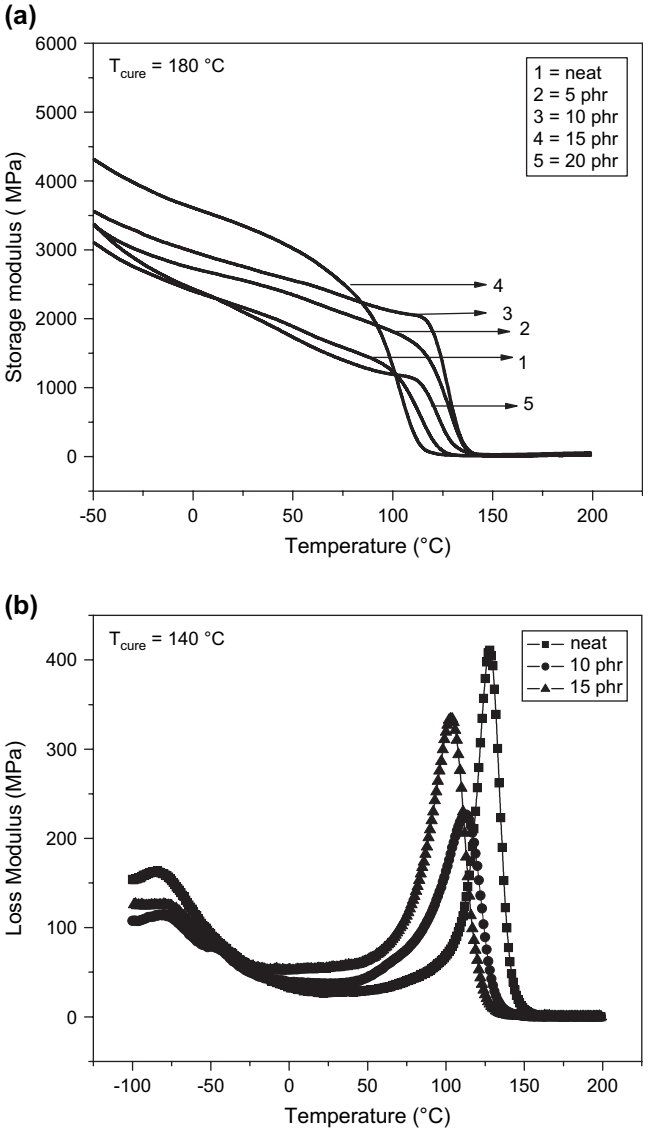

Fig. 17. (a) Storage modulus versus temperature of neat epoxy and blends at $T_{cure} = 180$ °C. (b) Loss modulus versus temperature of neat epoxy and modified blends at T_{cure}=140 °C.

6. Conclusion

A DGEBA-based epoxy resin was modified with a carboxyl-terminated butadiene and acrylonitrile copolymer using an anhydride hardener. The curing analysis was followed by DSC. The kinetic analysis was done by an autocatalytic model. The final stage of the reaction was analyzed by a diffusion control model. The physical transformations such as gelation and vitrification were examined and predicted. The addition of liquid rubber did not change the mechanism of cure. However, on lowering the temperature, the rate and the extent of reaction decreased. The extent of reaction decreased

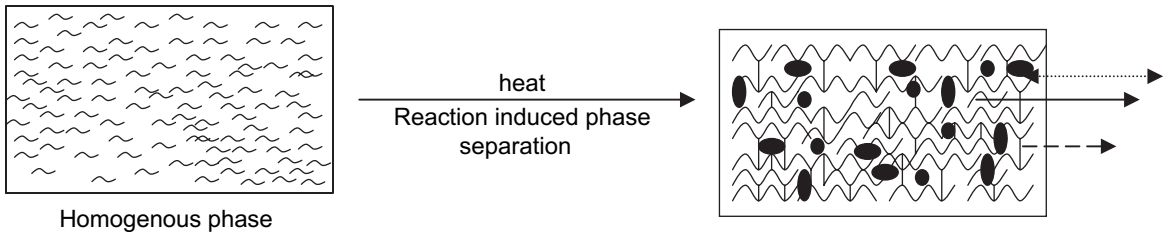

Fig. 16. A schematic representation of phase separated blend. The double-headed broken arrow represents CTBN-rich domains having dissolved epoxy phase. The solid arrow denotes epoxy-rich phase having dissolved CTBN phase. The dash type arrow shows cross-links in the epoxy matrix.

after attaining the gelation point. This was due to the phase separation of rubber from the epoxy matrix. Addition of a higher wt% of rubber decreases the rate and conversion. This was due to the dilution effect and increase in viscosity. Good fits are obtained between the autocatalytic model and the experimental data up to the vitrification state. Afterwards the reaction became diffusion controlled. The reaction during the later stages of cure was explained by introducing a diffusion factor, which agrees well with the kinetic data. The curic reaction mechanism by which the network structure of epoxy gets developed was discussed. The morphology development during cure was monitored by SEM studies. Phase separated morphology was obtained. Homogenous particle size distribution was observed for all blends. The SEM micrographs were quantified to find the size of the dispersed particles. The particle size was increased on the addition of CTBN and on lowering the curic temperature. The dynamic mechanical thermal analysis of the cured (neat) resin showed a reduction in the T_g value when T_{cure} was low. This is due to the lower conversion as a result of vitrification. The dynamic mechanical spectrum of the blends showed two T_gs corresponding to the modified-network and that of the rubber phase. The blends showed shifted T_gs on account of partial miscibility. The T_g of rubber phase was increased upon mixing with epoxy resin and that of the epoxy phase decreased. The storage modulus of the modified resin with a higher wt% of liquid rubber was lower corresponding to that of the neat resin, and that contain lower weight content of CTBN. This was due to the reduction in the cross-linking density and flexibilization of the epoxy network. The shifted T_gs clearly indicate that the phases are not pure.

Acknowledgements

One of the authors (Raju Thomas) thanks the Catholic University of Leuven, Belgium for analytical and financial support of the work. The authors would like to thank Huntsmann for the kind supply of chemicals for the study. Raju Thomas also thanks Kerala State Council for Science, Technology and Environment (KSCSTE) for SRS project.

References

[1] Bradleg TF. U.S. Patent; 1950. 449:2500.
[2] Caston P. U.S. Patent; 1943. 483:2324.
[3] Newey HA. U.S. Patent; 1958. 775:2264.
[4] Siebert AR. Rubber-modified thermoset resins. Adv. Chem. Series, vol. 208. Washington, DC; 1984. p. 179.
[5] Manzione LT, Gillham JK, McPherson CA. J Appl Polym Sci 1981; 26(889):907 and references cited therein.
[6] Kunz SC, Sayre JA, Assink RA. Polymer 1982;23:1897 and references cited therein.
[7] Riew CK, Gillham JK, editors. Adv. Chem. Series, vol. 208. Washington DC; 1984. p. 101.
[8] Riew CK, editor. Adv. Chem. Series, vol. 222; 1984.
[9] Paul NC, Richards DH, Thompson D. Polymer 1977;18:945.
[10] Baucer RS, editor. Epoxy Resin Chemistry 11. Washington, DC: ACS; 1983. p. 221.
[11] Bascom WD, Cottingham RL, Tones RL, Peyser P. J Appl Polym Sci 1979;19:2545.
[12] Smith RJM, Brekelmans WAM, Meijer HEH. J Mater Sci 2000;35:2855.
[13] Smith RJM, Brekelmans WAM, Meijer HEH. J Mater Sci 2000;35:2881.
[14] Henkee CS, Kramer EJ. J Polym Sci Polym Chem Ed 1984;22:721.
[15] ASTM E698-79, Annual book of ASTM standards, vol. 14; 1996. p. 2.
[16] Lange J, Altmann N, Kelley CT, Halley PJ. Polymer 2000;41:5949.
[17] Vergnaud JM, Bouzon J. Cure of thermosetting resins – modeling and experiments. London: Springer-Verlag; 1992.
[18] Calabrese L, Valenza A. Eur Polym J 2003;39:1355.
[19] Caly J, Sabra A, Pascault JP. Polym Eng Sci 1986;26:1514.
[20] Zukas WX. Polym Eng Sci 1989;29:1553.
[21] Rosu D, Mititelu A, Cascaval CN. Polym Test 2004;23:209.
[22] Francis B, Poel GV, Posada F, Groeninckx G, Rao VL, Ramaswamy R, et al. Polymer 2003;44:3687.
[23] Rosu D, Cascaval CN, Mustas F, Ciobanu C. Thermochim Acta 2002; 383(1–2):119.
[24] Nigel AJ, George AG. Polymer 1992;33(13):2679.
[25] Ma Z, Gao J. J Phys Chem B 2006;110:12380.
[26] Raman VI, Palmese GR. Macromolecules 2005;38:6923.
[27] Swier S, Assche GV, Vuchelen W, Mele BV. Macromolecules 2005;38: 2281.
[28] Becker O, Cheng YB, Varley RJ, Simon GP. Macromolecules 2003;36: 1616.
[29] Rebizant V, Venet AS, Tournilhac F, Pascault JP, Leibler L. Macromolecules 2004;37:8017.
[30] Kalogeras IM, Vassilikou-Dova A, Christakis I, Pietkiewicz D, Brostow W. Macromol Chem Phys 2006;207:879.
[31] Yin M, Zheng S. Macromol Chem Phys 2005;206:929.
[32] Opalicki M, Kenny JM, Nicholias L. J Appl Polym Sci 1996;61:1025.
[33] Gao J, Li Y. Polym Int 2000;49:1590.
[34] Martinez I, Martin MD, Eceiza A, Cyanguren P, Mondragon I. Polymer 2000;41:1027.
[35] Cracknell JG, Akay MJ. Therm Anal 1993;40:565.
[36] Kim BS, Chiba T, Inoue T. Polymer 1993;34:2809.
[37] Jenninger W, Schawe JEK, Alig I. Polymer 2000;41:1577.
[38] Fernandez B, Corcuera MA, Marieta C, Mondragon I. Eur Polym J 2001; 37:1863.
[39] Smith IT. Polymer 1961;2:95.
[40] Park SJ, Kim TJ, Lee JR. J Polym Sci Part B Polym Phys 2000;38:2114.
[41] Acitelli MA, Prime RB, Sacher E. Polymer 1971;12:335.
[42] Prime RB, Sacher E. Polymer (London) 1972;13:455.
[43] Prime RB. Polym Eng Sci 1973;13:365.
[44] Kamal MR. Polym Eng Sci 1974;14:23.
[45] Barral L, Cano J, Lopez AJ, Lopez J, Nogueira P, Ramirez C. J Appl Polym Sci 1995;56:1029.
[46] Ryan ME, Dutta A. Polymer 1979;20:203.
[47] Moroni A, Mijovic J, Pearce E, Foun C. J Appl Polym Sci 1986;32:3761.
[48] Kenny JM. J Appl Polym Sci 1994;51:761.
[49] Chern CS, Poehlein GW. Polym Eng Sci 1987;27:782.
[50] Khanna U, Chanda M. J Appl Polym Sci 1993;49:319.
[51] Rabinowitch E. Trans Faraday Soc 1937;33:1225.
[52] Karger-Kocsis J, Friedrich K. Compos Sci Technol 1993;48:263.
[53] Sayre JA, Assink RA, Lagasse RR. Polymer 1981;22:87.
[54] Thomas R, Abraham J, Thomas PS, Thomas S. J Polym Sci Part B Polym Phys 2004;42:2531.
[55] Eklind H, Maurer FHJ. J Polym Sci Phys Ed 1996;34:1569.
[56] Eklind H, Maurer FHJ. Polymer 1997;38:1047.